High-mass X-ray Binaries: Illuminating the Passage from Massive Binaries to Merging Compact Objects
Proceedings IAU Symposium No. 346, 2019
L. M. Oskinova, E. Bozzo, T. Bulik & D. Gies, eds.

doi:10.1017/S1743921319001236

Vertical distribution of HMXBs in NGC 55: Constraining their centre of mass velocity

Babis Politakis[1], **Andreas Zezas**[1,2,3], **Jeff J. Andrews**[2] **and Stephen J. Williams**[2,4]

[1]University of Crete, Department of Physics, Heraklion 71003, Greece
[2]Foundation for Research and Technology - Hellas (FORTH), Heraklion 71003, Greece
[3]Harvard-Smithsonian Center for Astrophysics, Cambridge, MA 02138
[4]USNO - 3450 Massachusetts Ave, NW, Washington, DC 20392-5420

Abstract. We analyse the vertical distribution of High Mass X-ray Binaries (HMXBs) in NGC 55, the nearest edge-on galaxy to the Milky Way. Our analysis reveals significant spatial offsets of HMXBs from the star forming regions, greater than those observed in the SMC and the LMC but similar with the Milky Way. The spatial offsets can be explained by a momentum kick the X-ray binaries receive during the formation of the compact object. The difference between the scale height of the vertical distribution of HMXBs and the vertical distribution of star-forming activity is 0.48±0.04 kpc. The centre-of-mass velocity of the distribution of HMXBs in NGC 55 is moving at a velocity of 52.4±11.4 km s^{-1}, greater than the corresponding velocity of HMXBs in the SMC and LMC, but consistent with velocities of Milky Way HMXBs.

Keywords. NGC 55, X-rays, HMXB

1. Introduction

High mass X-ray binaries (HMXBs) are among the brightest sources of X-ray emission in galaxies. The observed X-ray emission is powered either by accretion of wind material or mass transfer through stable Roche-lobe overflow from the companion star to the compact object. Although HMXBs are typically associated with star-forming regions (Grimm *et al.* 2003, Fabbiano 2006), there is observational evidence for a population of HMXBs that are somewhat offset from star-forming regions (Zezas *et al.* 2002). The observed displacement may be due to kicks after an asymmetric supernova explosion during the formation of the compact object (e.g. Fryer & Kalogera 1997). If they are large enough, kicks will extend the vertical distribution of HMXBs, which can potentially be measured in nearby edge-on galaxies such as NGC 55, the edge-on galaxy nearest the Milky Way, with high angular resolution X-ray telescopes. Although there are large quantities of gas off the disk plane forming structures such as HII regions, shells, knots and filaments (Otte & Dettmar 1999), due to the distance of NGC 55 (at 1.94 Mpc) the projected density of star-forming regions is too large to allow us to identify the possible birthplace of each individual HMXB. We therefore measure the displacement of HMXBs from the mid-plane of NGC 55 which is the region with the highest star-forming activity.

2. The HMXB population in NGC 55

The population of X-ray sources in NGC 55 has been analysed as part of the Chandra Local Volume Survey (Binder *et al.* 2015). The source list consists of 154 X-ray sources down to a flux of 7×10^{-16} erg s^{-1} cm^{-2}, classified by Binder *et al.* (2015) as: one as a Ultraluminous X-ray source (ULX), 65 as Active Galactic Nuclei (AGN), 10 as

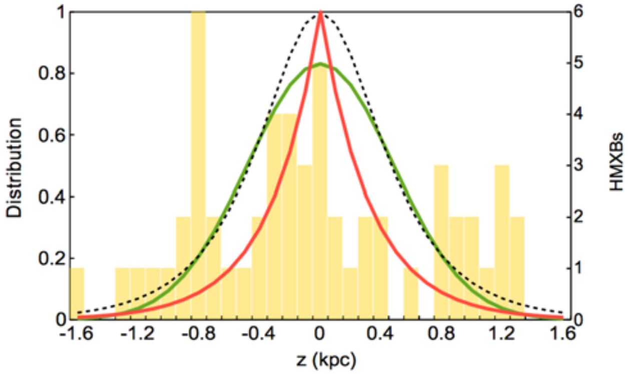

Figure 1. Simulated vertical distribution of HMXBs (dotted, black) from the mid-plane, as the convolution between a smearing of 0.48 kpc (green) on top of a star formation distribution of 0.33 kpc (red). The yellow histogram presents the observed vertical number density of HMXBs.

foreground stars, 11 as Supernova Remnants (SNRs) and 67 as X-ray binaries (XRBs) among which 24 as Low Mass X-ray binaries (LMXBs) and 43 as HMXBs. Based on our expectation of the AGN density in the Universe at our limiting X-ray sensitivity, we expect that 15 of the 67 sources classified as XRBs could be background AGN.

3. Vertical distribution of the HMXB population in NGC 55

We define the mid-plane of NGC 55 and measure the SFR density, by means of the highest resolution and least absorption-dependent SFR indicator we have available. This is the 8.0μm IRAC image that traces polycyclic aromatic hydrocarbon (PAH) emission from the star forming regions. We create a "star-formation" 8.0μm image by subtracting the 3.6μ m IRAC image from the 8.0μm image in order to remove the contribution from the non-star-forming, stellar populations. We then take slices with length equal to the major axis of NGC 55, at an angle equal to the position angle of NGC 55 and thickness equal to the FWHM of Spitzer's IRAC band 4 PSF. The slice with the highest surface brightness is selected as the mid-plane of NGC 55. We measure the vertical distribution of the SFR density calculated in bins parallel to the mid-plane. We then model the SFR density with an exponentially declining profile and fit the data to derive a star-formation scale height of $z_{\rm sfr}$=0.330±0.090 kpc (red line in Figure 1). The vertical number density of HMXBs is derived by measuring the number of HMXBs in bins of the same size as in the case of SFR (yellow histogram in Figure 1). The bins are finely spaced enough to capture the substantial displacement of HMXBs beyond the SFR density. The observed vertical displacement of HMXBs from their parent star-forming regions, may be due to kicks after an asymmetric supernova explosion during the formation of the compact object. We treat the contribution of kicks as a Gaussian smearing function of standard deviation σ that broadens the spatial distribution of HMXBs compared with their birth distribution. Based on the observed projected distances of HMXBs, we simulate the vertical distribution of HMXBs from the mid-plane as the convolution $C(\sigma,z_{\rm sfr},z)$ between this Gaussian and the exponential distribution of SFR with a scale height of $z_{\rm sfr}$=0.330 kpc:

$$C(\sigma, z_{\rm sfr}, {\rm z}) = \sqrt{\frac{\pi\sigma^2}{2}}\,\mathbf{exp}\left(\frac{\sigma^2}{2z_{\rm sfr}^2} - \frac{\rm z}{z_{\rm sfr}}\right) \times \left[\mathbf{erfc}\left[\sqrt{\frac{\sigma^2}{2}}\left(\frac{z}{\sigma^2} - \frac{1}{z_{\rm sfr}}\right)\right] - \mathbf{exp}\left(\frac{2{\rm z}}{z_{\rm sfr}}\right)\mathbf{erfc}\left[\sqrt{\frac{\sigma^2}{2}}\left(\frac{z}{\sigma^2} + \frac{1}{z_{\rm sfr}}\right)\right] - 2\right] \quad (3.1)$$

https://doi.org/10.1017/S1743921319001236 Published online by Cambridge University Press

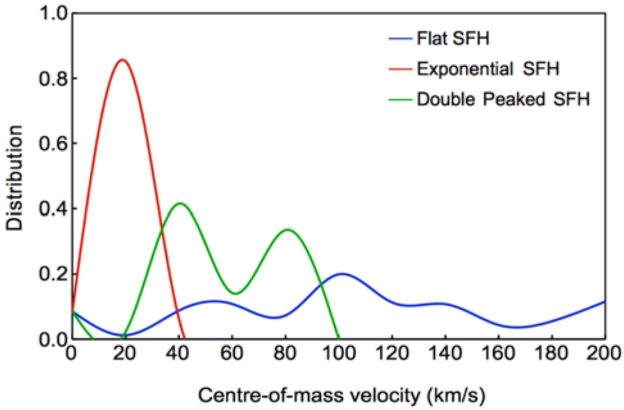

Figure 2. Distribution of the centre-of-mass transverse velocity for the HMXB population in NGC 55 for three different star-formation histories. The derived velocity depends strongly on the choice of the star-formation history adopted.

We apply the maximum likelihood method and find that the best estimate of the Gaussian smearing parameter σ is 0.48±0.04 kpc, which represents the scale height corresponding to the displacement between HMXBs and star-forming regions. Figure 1 shows the simulated vertical distribution of HMXBs (dotted, black) as a result of the convolution between a Gaussian smearing of 0.48 kpc (green) on top of a star formation distribution of 0.33 kpc (red).

We calculate the centre-of-mass transverse velocity of HMXBs by adopting HMXB travel times predicted by binary population synthesis codes for three different star formation history (SFH) models:

1. A flat SFH where stars are formed at a constant rate.
2. An exponentially declining SFH.
3. A double peaked exponentially declining SFH with bursts at 30 and 50 Myrs.

We select random offsets from the distribution of HMXBs (Figure 1) and divide them with random travel times from the distribution of SFH models. This gives the distribution of the centre-of-mass transverse velocity for the three different SFH models and is shown in Figure 2. We opt for the double peaked SFH model, in accordance with observations in star-forming galaxies that favour bursting star-formation models and estimate the centre-of-mass velocity of HMXBs in NGC 55 at 52.4±1.4 km s^{-1}. Similar measurements, show that the centre-of-mass velocities of HMXBs are lower at the MCs (12.4±7.0 km s^{-1} for the LMC, Antoniou & Zezas 2016 and 16 km s^{-1} for the SMC, Coe 2005) but similar in the Milky Way (42±14 km s^{-1}, van den Heuvel *et al.* 2000). We attribute the difference to the lack of information on the recent star formation history of NGC 55 (the value of the centre-of-mass velocity strongly depends on the choice of the star-formation history adopted), in contrast with the MCs where detailed SFH is available.

4. Vertical distribution of HMXBs in the MW

The HMXB population in our Galaxy provide an excellent benchmark for comparison with NGC55. We measure the positions of HMXBs with parallaxes available from the second data release of Gaia and fit the distribution of their vertical distances with an exponentially declining profile and find that the scale height of HMXBs in the Galaxy is h_z=145±23 kpc. The distribution of vertical distances of OB-stars from the Galaxy plane has a scale height of 103.1±3.0 (Kong & Zhu 2008). Therefore, the scale height corresponding to the displacement between HMXBs and star-forming regions in the Milky

https://doi.org/10.1017/S1743921319001236 Published online by Cambridge University Press

Way is $\sim$ 0.040±0.002 kpc, considerably lower than the corresponding scale height in NGC 55. We attribute this difference to the greater gravitational potential of the Galactic disk (the stellar mass of the MW is 25 times greater than the stellar mass of NGC 55) that confines HMXBs more closely to the Galactic plane.

References

Antoniou, V. & Zezas, A. 2016, *MNRAS*, 459, 528
Binder, B., Williams, B. F., Eracleous, M., *et al.* 2015, *AJ*, 150, 94
Blaauw, A. 1961,*BAIN*, 15, 265
Coe, M. J. 2005, *MNRAS*, 358, 1379
Fabbiano, G. 2006, *ARAA*, 44, 323
Fryer, C. & Kalogera, V. 1997, *ApJ*, 489, 244
Grimm, H.-J., Gilfanov, M. & Sunyaev, R. 2003, *MNRAS*, 339, 793
Kong, D.-L. & Zhu, Z. 2008, *Chinese Astronomy and Astrophysics*, 32, 360
Kudritzki, R. P., Castro, N., Urbaneja, M. A., *et al.* 2016, *ApJ*, 829, 70
Okazaki, A. T., Hayasaki, K. & Moritani, Y. 2013, *PASJ*, 65, 41
Otte, B. & Dettmar, R.-J. 1999, *A&A*, v.343, pp. 705-712
van den Heuvel, E. P. J., Portegies Zwart, S. F., Bhattacharya, D. & Kaper, L. 2000, *AAP*, 364, 563
Zezas, A., Fabbiano, G., Rots, A. H. & Murray, S. S. 2002, *ApJ*, 577, 710